# Rational Supershapes for Surface Reconstruction

Y.D. Fougerolle[1], A. Gribok[2], S. Foufou[1], F. Truchetet[1], and M.A. Abidi[2]
[1] Le2i Lab., UMR CNRS 5158, Dijon, University of Burgundy, France
[2] IRIS Lab. Knoxville, University of Tennessee, USA

## ABSTRACT

Simple representation of complex 3D data sets is a fundamental problem in computer vision. From a quality control perspective, it is crucial to use efficient and simple techniques do define a reference model for further recognition or comparison tasks. In this paper, we focus on reverse engineering 3D data sets by recovering rational supershapes to build an implicit function to represent mechanical parts. We derive existing techniques for superquadrics recovery to the supershapes and we adapt the concepts introduced for the ratioquadrics to introduce the rational supershapes. The main advantage of rational supershapes over standard supershapes is that the radius is now expressed as a rational fraction instead of sums and compositions of powers of sines and cosines, which allows simpler and faster computations during the optimization process. We present reconstruction results of complex 3D data sets that are represented by an implicit equation with a small number of parameters that can be used to build an error measure.

## 1. INTRODUCTION

Acquisition techniques of 3D models (scanners, sensors, etc.) usually produce huge data sets that cannot be easily compared. Among the possible techniques, a solution consists in defining an error function to represent a reference object. Several models have been used in the literature such as parametric surfaces, finite elements, level sets, and implicit functions. The approach presented in this paper belongs to the implicit surfaces approach, where we combine rational supershapes through R-functions to build a global implicit function that describes the model. Supershapes, also known as Gielis' surfaces, are a recent extension for superquadrics with rational and irrational symmetries. Superquadrics can be seen as spheres that are pinched or inflated using two shape coefficients to represent usual objects in modeling and engineering such as spheres, cubes, cylinders, diamonds and intermediate shapes. Gielis proposed an extension from superquadrics to supershapes by introducing rational and irrational symmetries.[1,2] Six shape coefficients are now considered to represent asymmetrical shapes. The symmetry parameters can be set to represent useful shapes such as the set of the regular polygons, which allows for a more general representation than superquadrics. Thanks to their ability to represent regular polygons and their various symmetries, supershapes are well suited for the representation of mechanical parts and have been used in literature to represent mechanical parts such as pistons, bolts, distributor caps, and more complex objects.[3,4]

There are few papers dedicated to supershape reconstruction in the literature.[5,6] Fortunately, superquadrics recovery has been widely studied in the literature. The most widely used techniques are based on the approaches proposed by Solina[7] and Jaklic,[8] where the problem is stated as an optimization problem of a suitable cost function. Usually, such a suitable cost function is built from the square of the implicit function, but other approaches, such as the one proposed by Gross *et al.*[9] introduced a radial cost function. In an experimental comparison of the most common cost functions in the literature, Zhang[10] concluded that standard cost functions, such as the ones used by Solina and Jaklic, were more appropriate to capture the dimensions of the object, whereas radial cost functions were more suitable to capture its shape. Optimizing a cost function for supershapes poses two main problems. First, the shape parameters are possibly not unique: a same shape can be described by several or even an infinite numbers of parameters sets. The second problem is due to the high non linearity of the cost function, which often presents many local minima. Similarly to the techniques proposed in[7,9,10] we apply the Levenberg-Marquardt algorithm to recover most of the parameters such as the shape, the orientation, the position, and the scale. Although the initial formulation of the supershapes introduced by Gielis allows for rational or irrational numbers of symmetry, the implicit functions proposed by Fougerolle *et al.*[3,4] require the symmetry numbers to be considered as integers. Symmetries can be efficiently detected and located by methods proposed by Sun *et al.*[11,12] that determine reflexion symmetries by using gradient information, or the approach

of Shen and Perry,[13] that uses generalized complex moments. Unfortunately, these methods are not well suited for our application since we only need the number of symmetries. Orientation and localization of symmetries will be handled during the optimization process. So, we use a simple heuristic that is based on measurements of sections of the object along its inertia axes to determine the number of symmetries.

The rest of the paper is as follows: the second section presents the parametric and implicit formulations of the supershapes, the third section deals with individual supershape reconstruction and the definition of a cost function to be minimized. The fourth section is dedicated to rational supershapes, that can be used as a simpler alternative to supershapes and that are simpler to reconstruct. The fifth section deals with R-functions to combine supershapes' implicit equations. We present in the sixth section our approach for multiple supershapes and holes reconstruction and an application to the reconstruction of real model. The last section is dedicated to our conclusions and future work.

The original contributions of this paper are an extension of superquadrics recovery techniques to supershapes, the introduction of rational supershapes, and the development of a reconstruction method based on the combination of individual supershape recovery and R-functions.

## 2. SUPERSHAPES

Supershapes have been introduced by Gielis as an extension of superquadrics with rational and irrational symmetries.[1,2] The radius of a 2D supershape, called a superpolygon, is parametrically defined by:

$$r(\theta) = \frac{1}{\sqrt[n_1]{\left|\frac{1}{a}\cos\left(\frac{m\theta}{4}\right)\right|^{n_2} + \left|\frac{1}{b}\sin\left(\frac{m\theta}{4}\right)\right|^{n_3}}}, \tag{1}$$

with $a$, $b$, and $n_i \in \mathbb{R}^+$. Parameters $a > 0$ and $b > 0$ control the size of the supershape. Extension to 3D is performed by the spherical product of two 2D supershapes similarly to superquadrics. For a unit supershape with natural number of symmetries $m$ and $M$, two implicit functions, presented in equations 2 and 3, have been proposed by Fougerolle *et al.*,[3,4] and are defined as:

$$F_1(x,y,z) = 1 - \frac{x^2+y^2+r_1^2(\theta)z^2}{r_1^2(\theta)r_2^2(\phi)}, \text{ and} \tag{2}$$

$$F_2(x,y,z) = 1 - \frac{1}{r_2(\phi)}\sqrt{\frac{x^2+y^2+z^2}{\cos^2\phi\,(r_1^2(\theta)-1)+1}}, \tag{3}$$

with angles $\theta$ and $\phi$ defined by:

$$\begin{cases} \theta = \theta(x,y) & = \arctan\left(\frac{y}{x}\right) \\ \phi = \phi(x,y,z,n_1,n_2,n_3) & = \arctan\left(\frac{zr_1(\theta)\sin(\theta)}{y}\right) \\ & = \arctan\left(\frac{zr_1(\theta)\cos(\theta)}{x}\right) \end{cases}.$$

The function $F_1$ is directly deduced from the 3D parametric formulation of supershapes and the function $F_2$ is an improvement of the previous function and is isotropic. The surface of a supershape is described by the locus where the potential field created is null, its inside where the field is positive and the outside where it is negative. Examples of supershapes are presente in figure 1.

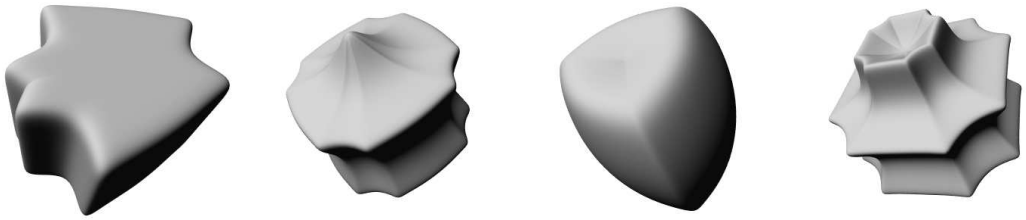

(a) (b) (c) (d)

**Figure 1.** Examples of supershapes for different shape parameters.

## 3. INDIVIDUAL SUPERSHAPE RECOVERY

The method introduced by Solina and Bajcsy[7] has been used in literature as a standard for superquadrics recovery. The problem is stated as an mean square optimization problem of a well chosen cost function. During an iterative process, the recovered supershape evolves to obtain a minimal value of the cost function. Another cost function, based on the notion of radial euclidian distance, has been introduced by Gross and Boult.[9] In an experimental comparison, Zhang *et al.*[10] conclude that the functions introduced by Solina are efficient to precisely capture the size of the object but are not as efficient as radial functions to capture the shape. Following these conclusions, we define a supershape cost function by:

$$Err\left(\Lambda\right) = a_1 a_2 a_3 \sum_{i=1}^{n} \left(F_2\left(P_i\right)\right)^2, \tag{4}$$

where $F_2(x, y, z)$ is the supershape radial implicit equation defined in equation 3. The introduction of the term $a_1 a_2 a_3$ is suggested by Solina *et al.* to maintain the reconstructed supershape to a minimal volume.

Since the implicit equations for supershapes require parameters $m$ and $M$ to be natural numbers, the Levenberg-Maquardt method cannot be applied because its needs to compute the gradient of the cost function. Sophisticated methods such as the ones proposed in[11–13] are not well adapted to our goals, because we only need the number of symmetries. Moreover, we deal with objects that may be noisy or incomplete, which would make harder to apply such methods. Fortunately, the nature of 3D supershapes can be used for a simpler symmetry number detection: the axis $(Oz)$ is a rotation symmetry axis, which implies for all orthogonal planar sections to this axis, that the symmetry number remains constant. So, by checking the number of extrema of the radius of planar sections of the object remains constant, we can approximately determine the symmetry numbers. For each planar section, in polar coordinates, the data can be represented as a curve $r(\theta)$, as illustrated on figure 2 and symmetry numbers correspond to the number of extrema of $r(\theta)$. For incomplete data, some data are missing and the curve is not continuous. We then work by intervals to locate potential extrema: we keep detected extrema on continuous intervals and we seek in other sections if there is any additional information to reconstruct the complete curve. After a full sweep of the data, the curve may still be incomplete and the symmetry numbers can not be precisely determined. In this case, we set $m$ and $M$ to 4 to make them transparent in the parametric formulation in Eq 1.

## 4. RATIONAL SUPERSHAPES

Supershape recovery involves to apply Levenberg-Marquardt method to iteratively make the supershape to evolve to represent the data with the minimal fitting error. During the process, the partial derivatives of the cost function defined in equation 4 are evaluated to determine the step to be added to the parameter vector. Due to the definition of the supershape radius, the partial derivatives are difficult to evaluate and may be very sensible for small parameter variations, which means the algorithm may be slow to converge or may converge to local minima. To reduce its sensibility, we introduce a new radius parameterization that is inspired by the work of Blanc and Schlick.[14] Blanc and Schlick replace power terms in the superquadrics equation by rational fractions, which means for $|t| < 1$ any term defined as

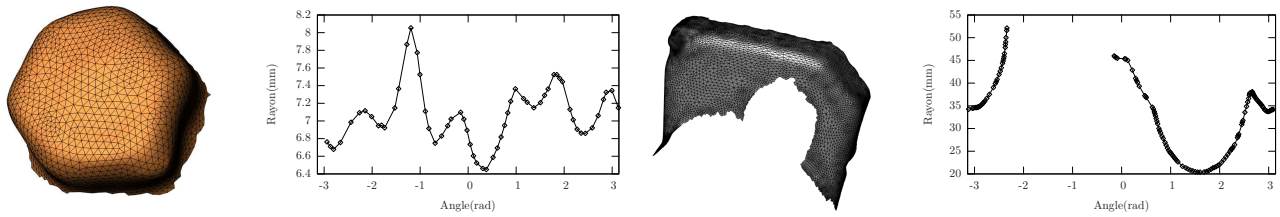


(a) (b) (c) (d)

**Figure 2.** Example of symmetry detection for incomplete data sets. a) and c) Initial data. b) and d) Curves $r = f(\theta)$ after a sweep along the data main inertia axis.

$$f_p(t) = |t|^p \tag{5}$$

is replaced by a rational fraction defined as

$$g_p(t) = \frac{|t|}{p + (1 - |t|)\, p}. \tag{6}$$

In our case, there are three power computations in equation 1 that can be replaced using this technique. By setting $U(\theta) = |\cos\frac{m\theta}{4}|$, $V(\theta) = |\cos\frac{m\theta}{4}|$ the radius defined in equation 1 can be rewritten as

$$r(\theta) = \frac{1}{(U^{n_2}(\theta) + V^{n_3}(\theta))^{\frac{1}{n_1}}}. \tag{7}$$

The terms $U^{n_2}(\theta)$ and $V^{n_3}(\theta)$ can be replaced by $\frac{U(\theta)}{n_2+(1-n_2)U(\theta)}$ and $\frac{V(\theta)}{n_3+(1-n_3)V(\theta)}$, respectively. By extracting a factor 2 to maintain the argument of the root to have a length smaller than 1 and by applying the same technique, we can express a new parametric form of the radius as a rational fraction defined by:

$$r(\theta) = 2^{\frac{-1}{n_1}} \left( \frac{1}{W(\theta)n_1} + 1 - \frac{1}{n_1} \right) \tag{8}$$

with $W(\theta)$ defined by

$$W(\theta) = \frac{U(\theta)}{n_2 + (1 - n_2)U(\theta)} + \frac{V(\theta)}{n_3 + (1 - n_3)V(\theta)}. \tag{9}$$

From our experiments, we obtain similar shapes for small shape coefficients, *i.e.* $n_i \in [1, 4]$ as illustrated in figure 3. For a same set of shape parameters, the rational supershape becomes rounder than a standard supershape as shape coefficients increase, as illustrated on figure 4. On these examples, we see rational supershapes and supershapes can represent similar shapes for small shape coefficients and can also present sharp features. Unfortunately, for high shape coefficient values, the resulting shapes are not similar. Nevertheless, a rational representation can be used in the early steps of the reconstruction algorithm to reduce the computation cost as long as the shape coefficients are not too important. During the reconstruction process, as soon as the difference between the supershape and the rational supershape becomes too important, or as soon as one or several shape coefficients increase, the initial supershape representation is used. This difference between shapes for important shape coefficients is a major difference when we compare superquadrics and ratioquadrics. While ratioquadrics can be used as a simpler alternative to superquadrics, rational supershapes can only be used as a way to reduce the computations during the early steps of our reconstruction algorithm.

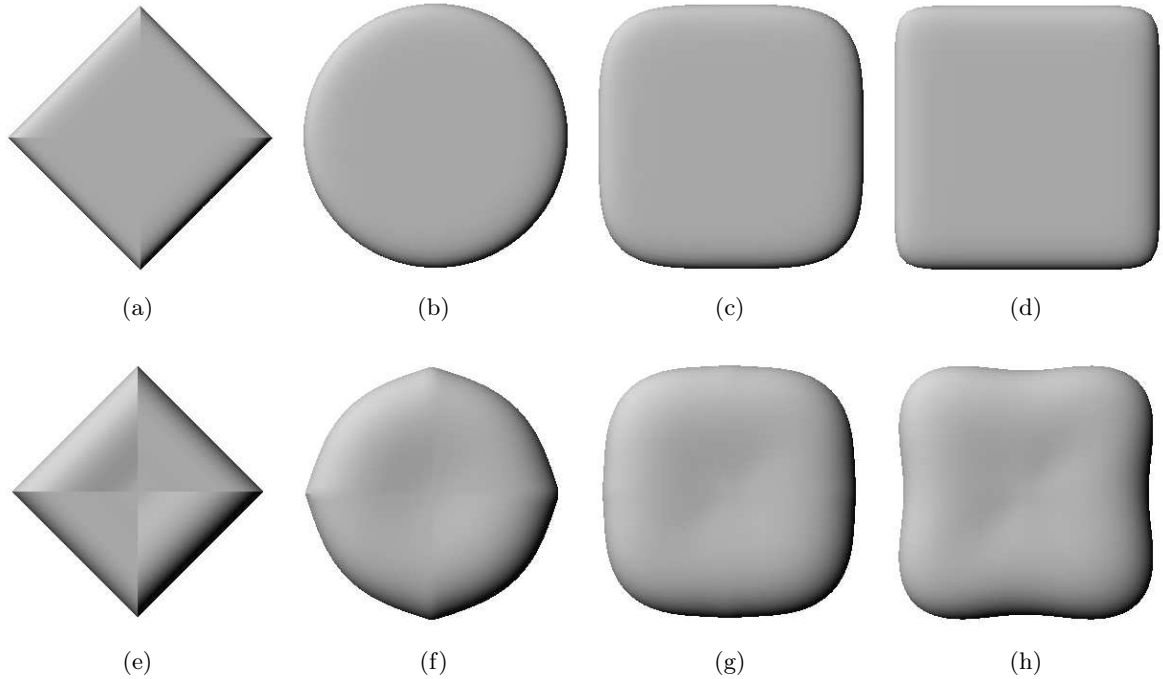


**Figure 3.** Examples of supershapes and ratio-supershapes generated for shape parameters $n = n_1 = n_2 = n_3$. a) and e) $n = 1$, b) and f) $n = 2$, c) and g) $n = 4$, d) and h) $n = 10$.

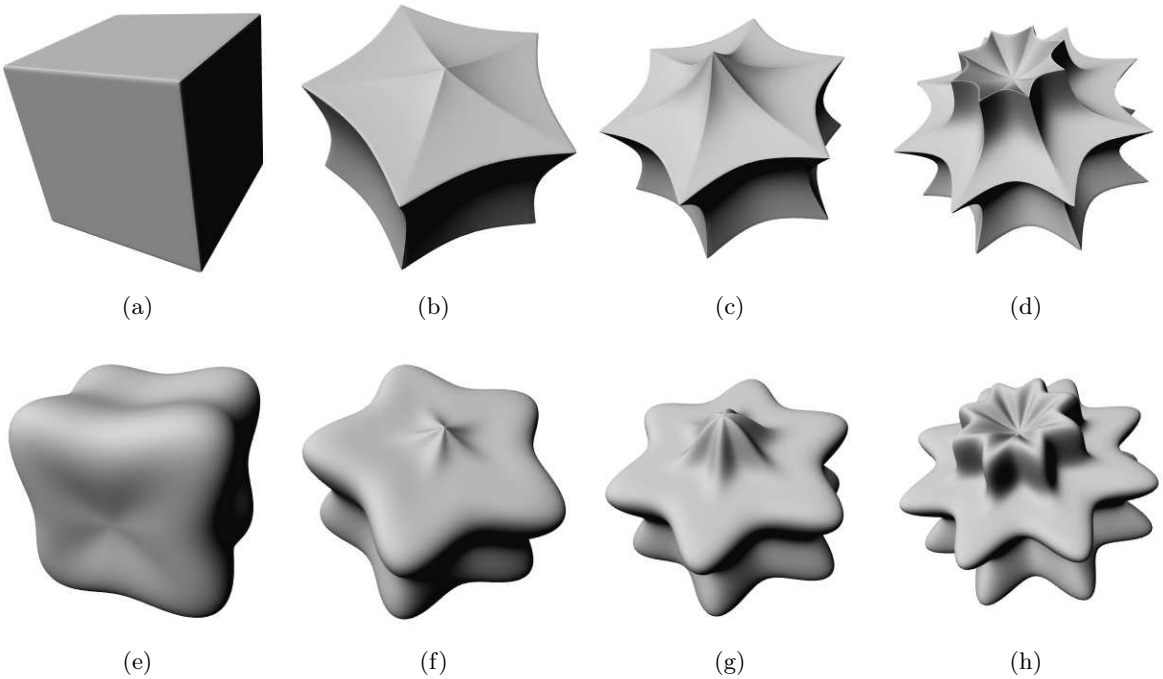


**Figure 4.** Examples of supershapes and ratio-supershapes generated for shape parameters $n_i = N_i = 100$ and various symmetry numbers. a) and e) $m = M = 4$, b) and f) $m = M = 5$, c) and g) $m = M = 6$, d) and h) $m = M = 8$.

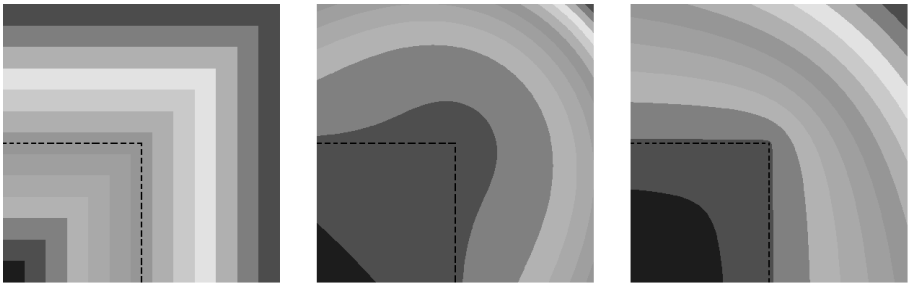

**Figure 5.** Intensity of the scalar field of the R-disjunction of two variables $x \in [-1, 1]$ and $y \in [-1, 1]$. In dashed line, the zero-set of the R-function. Left: $max(x, y)$, center: $R_0^m(x, y)$ with $m = 2$, and right: $R_p(x, y)$ with $p = 2$.

## 5. IMPLICIT MODELING AND R-FUNCTIONS

The primitives we consider have an implicit representation, which allows us to take advantage of implicit modeling techniques. For example, smooth objects can be generated using geometrically continuous blends, such as the ones introduced by Ricci[15] or Pasko.[16] Linear compositions can be used in reconstruction process, as proposed by DeCarlo *et al.*[17] In this category also fall R-functions, introduced by Rvachev.[18] An English tutorial has been proposed by Shapiro.[19] R-functions can be used to transcribe Boolean predicates into analytical equations, which allows to represent objects that are composed of several supershapes, may present holes, or may be composed of disjunct parts. We will denote R-conjunction and R-disjunction with the same notation (symbol $\pm$), with R-conjunction obtained by considering $-$ and R-disjunction by considering $+$. R-negation is the opposite sign function $\overline{x} \equiv -x$. Depending on their differential properties,[20] different R-funtions may be used, namely $R_\alpha$, $R_0^m$ and $R_p$. An illustration of R-disjunction using $R_\alpha$, $R_0^m$, and $R_p$ is presented in Fig. 5. $R_\alpha$ is defined as

$$R_\alpha : \frac{1}{1+\alpha}\left(x + y \pm \sqrt{x^2 + y^2 - 2\alpha xy}\right), \tag{10}$$

where $\alpha(f_1, f_2)$ is an arbitrary symmetric function such that $-1 < \alpha(f_1, f_2) \leq 1$. Setting $\alpha$ to 1 leads to the simplest and most popular R-functions $min(x, y)$ and $max(x, y)$.

To solve the loss of differentiability of the $R_\alpha$-function along the line $x = y$, two other R-functions $R_0^m$ and $R_p$ are proposed. $R_0^m$ is defined as

$$R_0^m : \left(x + y \pm \sqrt{x^2 + y^2}\right)\left(x^2 + y^2\right)^{\frac{m}{2}}, \tag{11}$$

where $m$ is any even positive integer. Shapiro shows in[20] that $R_0^m$ is $m$ times differentiable everywhere, including the corner point $x = y = 0$. All partial derivatives are identically zero at corner points, but unfortunately, $R_0^m$ is not normalized. $R_p$-function achieves normalization and is differentiable everywhere but at the corner point $x = y = 0$ and is defined as

$$R_p : x + y \pm \left(x^p + y^p\right)^{\frac{1}{p}}, \tag{12}$$

for any even positive integer $p$.

Two different aspects of our method require the use of R-functions. The first and most natural usage for R-function is the transcription of Boolean predicates into analytical equations. In our case, R-functions are applied to merge all the supershapes' implicit equations into a single analytical equation that implicitly describes the surface, the inside, and the outside of the whole object. Additionally, holes can be seen as negative objects that are represented by the intersection between an object to be dug and a reconstructed supershape. The second application of R-functions is the truncation of the supershapes to assert the reconstructed solid will be completely contained within the oriented bounding box of the data. The reconstructed object is defined as the union of several parts, each part being represented as a boolean composition of truncated supershapes and each

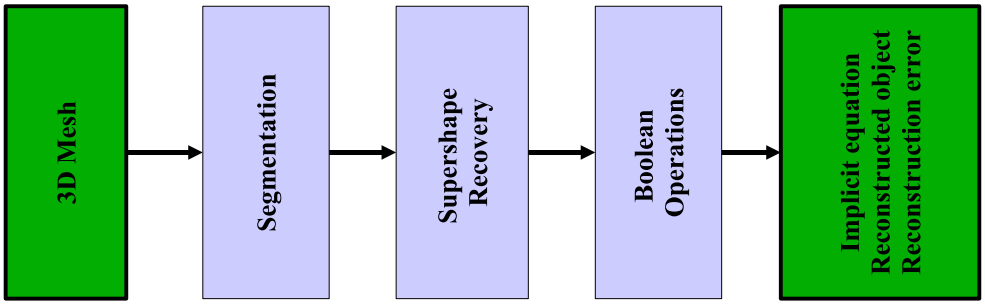


**Figure 6.** Reconstruction flowchart

truncated supershape as an intersection between two supershapes. Each truncated supershape is individually recovered from segmented parts of the data as presented in section 3. Finally, for each part, positive truncated supershapes are combined to build the envelop and negative supershapes to dig holes in it.

## 6. MULTIPLE SUPERSHAPE RECOVERY

We present a method to represent complex objects with several supershapes. Our algorithm proceeds in three steps, as illustrated in figure 6. The input is a segmented mesh by the technique proposed by Page *et al.*[21] and used by Zhang for superquadrics.[22] The output is a single implicit representation whose zero-set represents the surface of the whole reconstructed object. Since segmented data can be seen as the union of several parts, the union of the reconstructed parts can be transcribed into a single analytical equation using R-functions. In this paper we consider the $R_P$-function $R_{p=2}$.

### 6.1. Truncated supershapes and global error of fit

In the case of an object without hole, the final implicit function that corresponds to the union of all the truncated supershapes is defined by

$$F(P) = \bigvee_{j=1}^{p} f_{2_j}(P). \tag{13}$$

Terms $f_{2_j}$ correspond to the recovered truncated supershapes' implicit equations. Unfortunately, the union of reconstructed supershapes does not necessarily correspond exactly to the data: in some cases, some parts of the recovered supershapes have to be removed. To solve this problem, we define $f_{2_j}$ the implicit equation of a truncated supershape $j$ as the intersection between the reconstructed supershape $F_{2_j}$ and the oriented bounding box of its corresponding data $B_j$ by

$$f_{2_j}(P) = \left(F_{2_j} \wedge B_j\right)(P). \tag{14}$$

The global reconstruction error is derived from equation 4 and is defined by:

$$Err(\Lambda) = \sum_{i=1}^{n} \left( \bigvee_{j=1}^{p} \left(\sqrt{a_1 a_2 a_3}\right)_j \cdot f_{2_j}(P_i) \right)^2. \tag{15}$$

Once the parameters of the supershapes of the model are reconstructed, equation 15 can be used to determine similarity between a give 3D data set and the reconstructed reference model. Orientation, translation and scale parameters of the data can be optimized to minimize the cost function.

Truncated supershapes are necessary to avoid non desired parts to appear when the union of the supershapes. Approaches proposed by Solina and Bajcsy,[7] Jaklič *et al.*,[8] and Chevalier *et al.*[23] do not deal with this issue

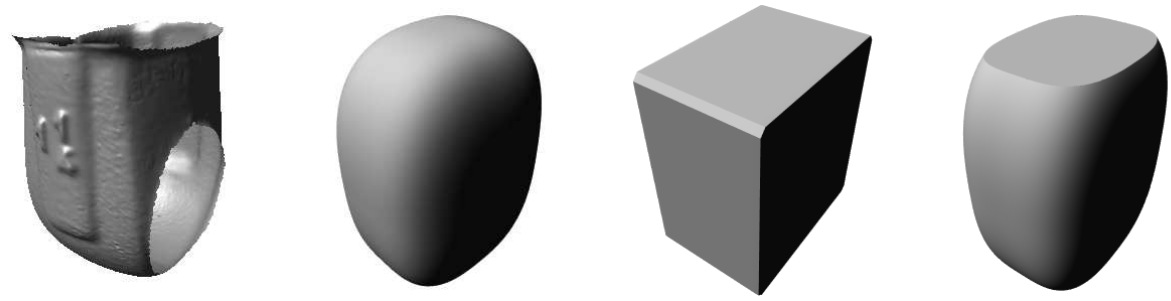

(a) (b) (c) (d)

**Figure 7.** Example of truncated supershape. a) Initial data, b) Reconstructed supershape, c) Bounding box, and d) Truncated supershape

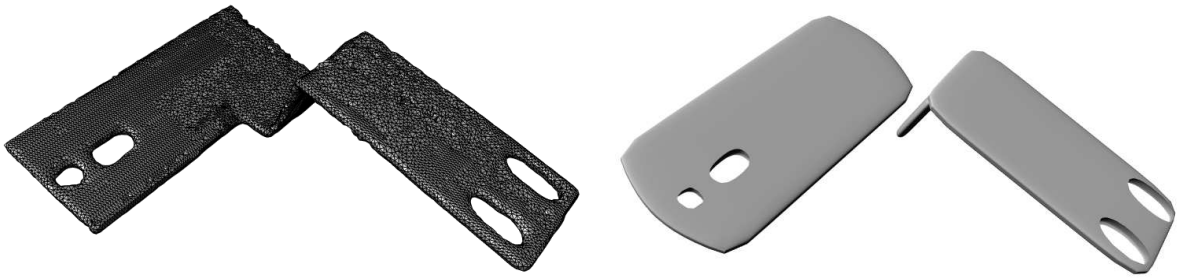

(a) (b)

**Figure 8.** Hole detection and reconstruction. a) Initial real data. b) Reconstructed surface.

because the reconstructed superquadrics are contained within the cloud of points during the reconstruction process. In our case, the pre-segmentation of the data implies the loss of the interior of the complete model, which requires to truncate the reconstructed supershape to represent only the segmented data, as illustrated on figure 7.

### 6.2. Reconstruction of objects with holes

Traditional approaches iteratively insert objects until a desired accuracy is reached, which often requires large number of superquadrics that are then fused using heuristics to simplify the final representation.[7,17,23] Similarly to the approach proposed by DeCarlo *et al.*,[17] we handle negative objects to represent holes and blending functions throught R-functions to allow topological changes of the reconstructed object. A hole can be seen as the intersection between an envelop and the outside of another object. To detect holes, we use the reconstruction error: points belonging to the borders of the cavity will introduce an important reconstruction error because they are located inside the reconstructed supershape. Such points are clustered into a secondary cloud of points to represent the cavity. We then deal with two data sets: the first corresponds to the envelop of the data, and the second to the hole that has to be reconstructed as illustrated in figure 8.

## 7. CONCLUSIONS

We have presented in this paper an application of supershapes and R-functions to surface recovery. We have introduced rational supershapes by expressing the 2D parametric radius of a supershape as a rational fraction. Although rational supershapes are simpler to optimize than supershapes, the shapes that are generated are similar only over a small shape coefficient interval, which restricts their usage to the first iterations of the reconstruction process. The surface reconstruction method presented in this paper is inspired from the techniques for superquadrics proposed by Solina and Bajcsy,[7] Gross and Boult,[9] Zhang *et al.*,[22] Jaklič *et al.*,[8] and Chevalier

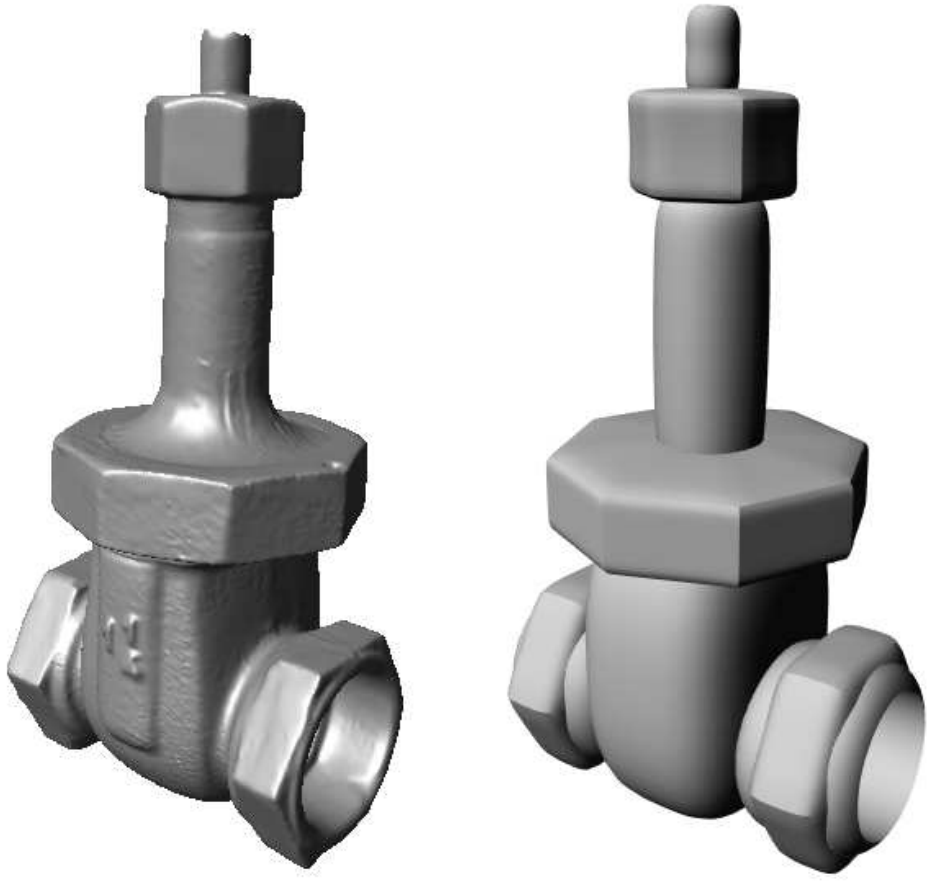

(a) (b)

**Figure 9.** Complex Object reconstruction. a) Initial real data. b) Reconstructed surface.

*et al.*[23] We proposed a cost function based on a radial implicit function of supershapes and a simple heuristic to detect symmetry numbers to reconstruct truncated individual supershape with minimal volume. Using R-functions, we obtain one global reconstruction error to characterize the final result and the representation can handle holes and topological changes during the optimization process. By comparison with superquadrics, several aspects require further investigations: if supershapes can represent a wider set of shapes than superquadrics, they are more complicated to reconstruct using a determinist algorithm such as the Levenberg-Marquardt method. Moreover, it would be interesting to investigate the direct optimization of the resulting R-function to make all the supershapes to evolve at each iteration of the algorithm, but the parameter space dimensions quickly become important, which raises questions about the convergence of the algorithm and the choice of the primitives or the choice of the optimization method. In future work we are going to investigate potential solutions to directly optimize such a cost function based on R-function of supershapes using non determinist algorithm such as genetic algorithm, the Nelder-Mead algorithm or simulated annealing.

## REFERENCES


1. J.Gielis, "A generic geometric transformation that unifies a wide range of natural and abstract shapes," *American Journal of Botany* **90**, pp. 333–338, 2003.
2. J. Gielis, B. Beirinckx, and E. Bastiaens, "Superquadrics with rational and irrational symmetry," in *Proceedings of the Eighth ACM Symposium on Solid Modeling and Applications 2003*, pp. 262–265, (Seattle, Washington, USA), June 2003.

3. Y. D. Fougerolle, A. Gribok, S. Foufou, F. Truchetet, and M. A. Abidi, "Boolean operations with implicit and parametric representation of primitives using R-functions," *IEEE Transactions on Visulisation and Computer Graphics* **11**(5), pp. 529–539, 2005.
4. Y. D. Fougerolle, A. Gribok, S. Foufou, F. Truchetet, and M. A. Abidi, "Implicit surface modeling using supershapes and R-functions," in *Proc. Pacific Graphics'05*, pp. 169–172, (Macao, China), October 2005.
5. Y. D. Fougerolle, A. Gribok, S. Foufou, F. Truchetet, and M. A. Abidi, "Radial supershapes for solid modeling," *J. Computer and Science Technology* **21**(2), pp. 238–243, 2005.
6. Y. D. Fougerolle, A. Gribok, S. Foufou, F. Truchetet, and M. A. Abidi, "Supershape recovery from 3D data sets," in *Proc. IEEE International Conference on image Processing*, pp. 2193–2196, (Atlanta, GA), October 2006.
7. F. Solina and R. Bajcsy, "Recovery of parametric models from range images: The case for superquadrics with global deformations," *The Visual Computer* **12**(2), pp. 131–1476, 1990.
8. A. Jaklič, A. Leonardis, and F. Solina, *Segmentation and recovery of superquadrics*, Kluwer Academic Publisher, Dordrecht, 2000.
9. A. Gross and T. Boult, "Error of fit measures for recovering parametric solids," in *Proc. Internat. Conf. Computer Vision*, pp. 690–694, 1988.
10. Y. Zhang, "Experimental comparison of superquadric fitting objective functions," *Pattern Recognition Letter* **24**, pp. 2185–2193, 2003.
11. C. Sun and D. Si, "Fast reflectional symmetry detection using orientation histograms," *Journal of Real-Time Imaging* **5**(1), pp. 63–74, 1999.
12. C. Sun and J. Sherrah, "3-D symmetry detection using the extended gaussian image," *IEEE Transactions on Pattern Analysis and Machine Intelligence* **19**(2), pp. 164–168, 1997.
13. D. Shen, H. Ip, K. Cheung, and E. Teoh, "Symmetry detection by generalized complex (GC) moments: a close-form solution," *IEEE Pattern Analysis And Machine Intelligence* **21**(5), pp. 466–476, 1999.
14. C. Blanc and C. Schlick, "Ratioquadrics: an alternative model for superquadrics," *The Visual Computer* **12**(8), pp. 420–428, 1996.
15. A. Ricci, "A constructive geometry for computer graphics," *The Computer Journal* **16**(2), pp. 157–160, 1972.
16. A. Pasko, V. Adzhiev, A. Sourin, and V. Savchenko, "Function representation in geometric modeling: concepts, implementation and applications," *The Visual Computer* **11**(8), pp. 429–446, 1995.
17. D. DeCarlo and D. Metaxas, "Shape evolution with structural and topological changes using blending," *IEEE Transactions on Pattern Analysis and Machine Intelligence* **20**, pp. 1186–1205, 1998.
18. V. L. Rvachev, *Geometric Applications of Logic Algebra*, Naukova Dumka, 1967. In Russian.
19. V. Shapiro, "Theory of R-functions and applications: A primer," Tech. Rep. TR91-1219, Computer Science Department, Cornell University, Ithaca, NY, 1991.
20. V. Shapiro and I. Tsukanov, "Implicit functions with guaranteed differential properties," in *Symposium on Solid Modeling and Applications*, pp. 258–269, 1999.
21. D. Page, *Part Decomposition of 3D Surfaces*. PhD thesis, University of Tennessee, May 2003.
22. Y. Zhang, *superquadric representation of scenes from multi-view range data*. PhD thesis, University of Tennessee, December 2004.
23. L. Chevalier, F. Jaillet, and A. Baskurt, "Segmentation and superquadric modeling of 3D objects.," in *Proc. of WSCG*, February 2003.